Time Domain Computational Modelling of 1D Arterial Networks in Monochorionic Placentas.

Victoria E. Franke[1], Kim H. Parker[2], Ling Y. Wee[3], Nicholas M. Fisk[3], Spencer J. Sherwin[1]

[1]Biomedical Flow Group, Department of Aeronautics,
Imperial College London, South Kensington Campus
London SW7 2AZ, U.K.
e-mail: v.shenton@imperial.ac.uk, s.sherwin@imperial.ac.uk,
web page: http://www.ae.imperial.ac.uk/staff/sherwin

[2] Department of Bioengineering.

[3] Institute of Reproductive and Developmental Biology,
Imperial College London at Queen Charlotte's Hospital,
Hammersmith Campus.

Abstract

In this paper we outline the hyperbolic system of governing equations describing one-dimensional blood flow in arterial networks. This system is numerically discretised using a discontinuous Galerkin formulation with a spectral/*hp* element spatial approximation. We apply the numerical model to arterial networks in the placenta. Starting with a single placenta we investigate the velocity waveform in the umbilical artery and its relationship with the distal bifurcation geometry and the terminal resistance. We then present results for the waveform patterns and the volume fluxes throughout a simplified model of the arterial placental network in a monochorionic twin pregnancy with an arterio-arterial anastomosis and an arterio-venous anastomosis. The effects of varying the time period of the two fetus' heart beats, increasing the input flux of one fetus and the role of terminal resistance in the network are investigated and discussed. The results show that the main features of the in-vivo, physiological waves are captured by the computational model and demonstrate the applicability of the methods to the simulation of flows in arterial networks.

1 Introduction

Pressure and blood flow waveforms in the human body can be recorded using techniques such as catheter mounted manometers and Doppler ultrasound. These measurements, combined with the observation that abnormal waveforms in arteries may indicate a pathological state, provide a means for diagnosing various ailments in clinical practice.

The physiological properties of blood flow in arterial networks can be reasonably approximated by a one-dimensional model, where the blood velocity, pressure and vessel wall properties are assumed to be constant across a section [9, 10, 6]. The fundamental equations of conservation of mass and momentum lead to a hyperbolic conservation law describing the propagation of waves within the networks. Solving this system computationally using spectral/*hp* elements offers a numerically tractable method of modelling the pressure and velocity waveforms in the larger vessels of arterial networks, which can then be compared with in-vivo measurements made in clinical settings. In this paper an application of the one-dimensional model is investigated: modelling of fetoplacental circulations. This is of particular interest in twin pregnancies when a single placenta is shared between the two fetuses (monochorionic twin pregnancies). In these cases the fetoplacental circulations may be linked by anastomoses between arteries and arteries, arteries and veins or more rarely veins and veins. Connections of these types result in an unbalanced transfusion of blood from one fetus (the donor) to the other (the recipient), which can adversely affect the development of the fetuses, can lead to a condition known as Twin-to-twin transfusion syndrome (TTTS) and may even be fatal.

The paper is organised as follows. In section 2 we outline the hyperbolic system of governing equations and its numerical discretisation using the discontinuous Galerkin method with a one-dimensional spectral/*hp* element spatial approximation. In section 3 we demonstrate the application of the model to fetoplacental circulations. We start by considering in section 3.3 the modelling of the arterial network

in a single placenta and then in section 3.4 we extend the results to a simplified model of an arterial network in a monochorionic twin pregnancy. Finally, the results are summarised and conclusions are drawn in section 4.

2 Governing Equations and Numerical Discretisation

The human arteries can be thought of as distensible tubes. Assuming static equilibrium in the radial direction of a cylindrical tube, averaging the blood velocity across the section and neglecting the curvature of the arteries, the system can be reduced to a one-dimensional problem. The equations representing continuity of mass and momentum can then be written as:

$$\frac{\partial A}{\partial t} + \frac{\partial Au}{\partial x} = 0 \tag{1}$$

$$\frac{\partial u}{\partial t} + u\frac{\partial u}{\partial x} = -\frac{1}{\rho}\frac{\partial p}{\partial x} \tag{2}$$

where the x is the axial direction, $A = A(x,t)$ is the cross sectional area of the blood vessel, $u = u(x,t)$ is the blood velocity averaged across the section and $\rho = const$ is the density of the blood. The relationship between the blood pressure, p, and area, A, is approximated using Laplace's law, i.e.

$$p = p_{ext} + \beta(\sqrt{A} - \sqrt{A_0}), \tag{3}$$

where for a thin walled vessels

$$\beta = \beta(x) = \frac{\sqrt{\pi}h_0 E}{A_0}.$$

In the above $h_0 (= h_0(x))$ and $A_0 = (A_0(x))$ denote the vessel wall thickness and cross-sectional area at the equilibrium state, $E = E(x)$ is the Young modulus and p_{ext} is the external pressure on the artery.

A high order discontinuous Galerkin formulation with a 1D spectral/hp element spatial approximation is applied to solve the system of equations within each vessel, as explained in section 2.2.

At the bifurcations between vessels there are discontinuities in u, A and the material properties leading to a Riemann problem. This can be solved numerically using the characteristic form of the hyperbolic system combined with the assumptions of conservation of mass and total pressure at the junction. These are also governing equations of our system and therefore before discussing the numerical implementation we outline the characteristic system.

2.1 Characteristic System

To write the system of equations (1) and (2) in the characteristic form the chain rule is applied to the pressure-area relationship, equation (3) to give:

$$\frac{\partial p}{\partial x} = \frac{\partial p}{\partial A}\frac{\partial A}{\partial x} + \frac{\partial p}{\partial \beta}\frac{\partial \beta}{\partial x} + \frac{\partial p}{\partial A_0}\frac{\partial A_0}{\partial x}$$

where

$$\frac{\partial p}{\partial A} = \frac{\beta}{2\sqrt{A}}.$$

by simple manipulations the system of equations (1) and (2) can be written in a non-conservative form as follows:

$$\frac{\partial \boldsymbol{U}}{\partial t} + \boldsymbol{H}\frac{\partial \boldsymbol{U}}{\partial x} = \begin{bmatrix} A \\ u \end{bmatrix}_t + \begin{bmatrix} u & A \\ c^2/A & u \end{bmatrix}\begin{bmatrix} A \\ u \end{bmatrix}_x = \begin{bmatrix} 0 \\ f \end{bmatrix} \tag{4}$$

where

$$c^2 = \frac{A}{\rho}\frac{\partial p}{\partial A} = \frac{\beta A^{1/2}}{2\rho} \text{ and } f = \frac{1}{\rho}\left[-\frac{\partial p}{\partial \beta}\frac{\partial \beta}{\partial x} - \frac{\partial p}{\partial A_0}\frac{\partial A_0}{\partial x}\right].$$

Matrix $\boldsymbol{H}$ has two real eigenvalues $\lambda_{1,2} = u \pm c$ and the corresponding eigenmatrix $\boldsymbol{Q}$ is:

$$\boldsymbol{Q} = \left[\begin{array}{c} \boldsymbol{q_1}, \boldsymbol{q_2} \end{array} \right] = \gamma \left[\begin{array}{cc} A & -A \\ c & c \end{array} \right] \tag{5}$$

where γ is an arbitrary scaling factor.

If $\boldsymbol{HQ} = \boldsymbol{Q\Lambda}$ then the matrix $\boldsymbol{H} = \boldsymbol{Q\Lambda Q}^{-1}$, where $\boldsymbol{\Lambda}$ is the diagonal matrix formed by the eigenvalues of $\boldsymbol{H}$. Substituting this into equation (4), assuming $f = 0$ (i.e. no variation in β or A_0 along the vessel), and premultiplying by $\boldsymbol{Q}^{-1}$ gives:

$$\boldsymbol{Q^{-1}} \frac{\partial \boldsymbol{U}}{\partial t} + \boldsymbol{\Lambda Q}^{-1} \frac{\partial \boldsymbol{U}}{\partial x} = 0 \tag{6}$$

If there exists a quantity $\boldsymbol{W} = \boldsymbol{W}(\boldsymbol{U})$ such that:

$$\frac{\partial \boldsymbol{W}}{\partial \boldsymbol{U}} = \boldsymbol{Q}^{-1} \tag{7}$$

then the characteristic variables can be determined by integrating the differential system:

$$\boldsymbol{Q}^{-1} = \gamma \left[\begin{array}{cc} \frac{1}{2A} & \frac{1}{2c} \\ -\frac{1}{2A} & \frac{1}{2c} \end{array} \right] = \frac{\partial \boldsymbol{W}}{\partial \boldsymbol{U}} = \gamma \left[\begin{array}{cc} \frac{\partial W_1}{\partial A} & \frac{\partial W_1}{\partial u} \\ \frac{\partial W_2}{\partial A} & \frac{\partial W_2}{\partial u} \end{array} \right] \tag{8}$$

A possible choice for γ where the characteristic variables satisfy the analytic condition ($\frac{\partial^2 W_{1,2}}{\partial A \partial u} = \frac{\partial^2 W_{1,2}}{\partial u \partial A}$) condition is $\gamma = 2c$, since A does not depend on u. Therefore if the characteristic variables exist they must satisfy:

$$\frac{\partial W_1}{\partial A} = \frac{c}{A}, \qquad \frac{\partial W_1}{\partial u} = 1, \tag{9}$$

$$\frac{\partial W_2}{\partial A} = -\frac{c}{A}, \qquad \frac{\partial W_2}{\partial u} = 1 \tag{10}$$

Integrating the differential form in equations (9) and (10) we obtain:

$$W_1 = u + \int_{A_0}^{A} \frac{c(A)}{A} dA = u + 4c = u + 4\sqrt{\frac{\beta}{2\rho}} A^{1/4}, \tag{11}$$

$$W_2 = u - \int_{A_0}^{A} \frac{c(A)}{A} dA = u - 4c = u - 4\sqrt{\frac{\beta}{2\rho}} A^{1/4} \tag{12}$$

Since $\beta > 0$, we may write, as previously reported in [4], the variables (A, u) in terms of (W_1, W_2) as:

$$A = \left[\frac{(W_1 - W_2)}{4} \right]^4 \left(\frac{\rho}{2\beta} \right)^2, \qquad u = \frac{(W_1 + W_2)}{2}. \tag{13}$$

Using the relation in equation (7), equation (6) can be transformed into a decoupled system of equations for the characteristic variables, which component-wise is:

$$\frac{\partial W_1}{\partial t} + \lambda_1 \frac{\partial W_1}{\partial x} = 0, \tag{14}$$

$$\frac{\partial W_2}{\partial t} + \lambda_2 \frac{\partial W_2}{\partial x} = 0. \tag{15}$$

2.2 Discontinuous Galerkin Method

The wave propagation speeds in the large arteries are typically an order of magnitude higher than the average flow speeds, hence the characteristic system is subcritical (i.e. $\lambda_1 > 0$ and $\lambda_2 < 0$). Further, under physiological conditions shock waves will not be present in the system and hence the solutions will be smooth. For continuous solutions of this type high-order methods are particularly attractive due to the fast convergence of the phase and diffusion properties with order of the scheme [11]. The discontinuous Galerkin method is an appealing formulation for the high-order discretisation of the conservation laws as it propagates waves with minimal numerical diffusion and dispersion for many periods. Following the work of Cockburn and Shu [1] and Lomtev, Quillen and Karniadakis [7] we proceed as follows.

The one-dimensional hyperbolic system, equations (1) and (2), can be expressed in a conservative form:

$$\frac{\partial \boldsymbol{U}}{\partial t} + \frac{\partial \boldsymbol{F}}{\partial x} = 0 \tag{16}$$

where

$$\boldsymbol{U} = \begin{bmatrix} U_1 \\ U_2 \end{bmatrix} = \begin{bmatrix} A \\ u \end{bmatrix} \qquad \boldsymbol{F} = \begin{bmatrix} F_1 \\ F_2 \end{bmatrix} = \begin{bmatrix} uA \\ \frac{u^2}{2} + \frac{p}{\rho} \end{bmatrix}.$$

To solve this system in a domain $\Omega = (a, b)$ discretized into a mesh of N_{el} elemental non-overlapping regions $\Omega_e = (x_e^l, x_e^u)$, such that $x_e^u = x_{e+1}^l$ for $e = 1, \ldots, N_{el}$, and

$$\bigcup_{e=1}^{N_{el}} \overline{\Omega}_e = \overline{\Omega},$$

we start by constructing the weak form of (16), i.e.:

$$\left(\frac{\partial \mathbf{U}}{\partial t}, \boldsymbol{\psi}\right)_\Omega + \left(\frac{\partial \mathbf{F}}{\partial x}, \boldsymbol{\psi}\right)_\Omega = 0 \qquad i = 1, 2 \tag{17}$$

where

$$(\boldsymbol{u}, \boldsymbol{v})_\Omega = \int_\Omega \boldsymbol{u}\ \boldsymbol{v}\ dx.$$

is the standard $\boldsymbol{L}^2(\Omega)$ inner product. Decomposing the integral into elemental regions we obtain:

$$\sum_{e=1}^{N_{el}} \left[\left(\frac{\partial \mathbf{U}}{\partial t}, \boldsymbol{\psi}\right)_{\Omega_e} + \left(\frac{\partial \mathbf{F}}{\partial x}, \boldsymbol{\psi}\right)_{\Omega_e} \right] = 0. \tag{18}$$

Integrating the second term by parts leads to:

$$\sum_{e=1}^{N_{el}} \left(\frac{\partial \mathbf{U}}{\partial t}, \boldsymbol{\psi}\right)_{\Omega_e} - \left(\mathbf{F}, \frac{d\boldsymbol{\psi}}{dx}\right)_{\Omega_e} + \left[\boldsymbol{\psi} \cdot \mathbf{F}\right]_{x_e^l}^{x_e^u} = 0 \tag{19}$$

To get the discrete form of our problem we choose $\mathbf{U}$ to be in the finite space of $\boldsymbol{L}^2(\Omega)$ functions which are polynomial of degree P on each element and indicate an element of such space using the superscript δ. We also note that $\mathbf{U}^\delta$ may be discontinuous across inter-element boundaries. However to attain a global solution in the domain Ω we need to allow information to propagate between the elemental regions. Information is propagated between elements by upwinding the boundary flux in the third term of equation (19). Denoting the upwinded flux as $\mathbf{F}^u$, the discrete weak formulation can now be written as:

$$\sum_{e=1}^{N_{el}} \left(\frac{\partial \mathbf{U}^\delta}{\partial t}, \boldsymbol{\psi}^\delta\right)_{\Omega_e} - \left(\mathbf{F}(\mathbf{U}^\delta), \frac{d\boldsymbol{\psi}^\delta}{dx}\right)_{\Omega_e} + \left[\boldsymbol{\psi}^\delta \cdot \mathbf{F}^u\right]_{x_e^l}^{x_e^u} = 0, \tag{20}$$

Following the traditional Galerkin approach, we choose the test function within each element to be in the same discrete space as the numerical solution $\mathbf{U}^\delta$. At this point if we define our polynomial basis and choose an appropriate quadrature rule we would now have a semi-discrete scheme. However, from an

implementation point of view, the calculation of the second term can be inconvenient and consequently we choose to integrate this term by parts once more to obtain:

$$\sum_{e=1}^{N_{el}} \left(\frac{\partial \mathbf{U}^\delta}{\partial t}, \boldsymbol{\psi}^\delta \right)_{\Omega_e} + \left(\frac{\partial \mathbf{F}(\mathbf{U}^\delta)}{\partial x}, \boldsymbol{\psi}^\delta \right)_{\Omega_e} + \left[\boldsymbol{\psi}^\delta \cdot \left[\mathbf{F}^u - \mathbf{F}(\mathbf{U}^\delta) \right] \right]_{x_e^l}^{x_e^u} = 0. \tag{21}$$

We note that the information between elements is transmitted by the third boundary term as the difference between the upwinded and the local fluxes, $\left[\boldsymbol{\psi}^\delta \cdot \left[\mathbf{F}^u - \mathbf{F}(\mathbf{U}^\delta) \right] \right]_{x_e^l}^{x_e^u}$. This method can be considered as a penalty method with an automatic procedure for determining the penalty parameter.

Finally we select our expansion basis to be a polynomial space of order P and expand our solution on each element e in terms of Legendre polynomials $L_p(\xi)$, i.e.:

$$\mathbf{U}^\delta\big|_{\Omega_e}(x_e(\xi), t) = \sum_{p=0}^{P} L_p(\xi) \hat{\mathbf{U}}_e^p(t).$$

where, following standard finite element techniques, we consider ξ in the reference element $\Omega_{st} = \{-1 \leq \xi \leq 1\}$ and introduce the elemental affine mapping:

$$x_e(\xi) = x_e^l \frac{(1-\xi)}{2} + x_e^u \frac{(1+\xi)}{2}.$$

We note that the choice of discontinuous discrete solution and test functions allows us to decouple the problem on each element, the only link coming through the upwinded boundary fluxes. Orthonormal Legendre polynomials are particularly convenient, because the basis is orthogonal with respect to the $\boldsymbol{L}^2(\Omega_e)$ inner product, and equation (21) turns out to be equivalent to solving, component-wise, for all elements e:

$$J_e \frac{\partial \hat{U}_{i,e}^p}{\partial t} = -J_e \left(\frac{\partial F_i}{\partial x}, L_p \right)_{\Omega_e} - \left[L_p \left[F_i^u - F_i(\mathbf{U}^\delta) \right] \right]_{x_e^l}^{x_e^u} = 0, \quad p = 1, \ldots, P, \quad i = 1, 2 \tag{22}$$

where J_e is the Jacobian of the elemental mapping, $J_e = \frac{1}{2}(x_e^u - x_e^l)$. To complete the discretisation we require a time integration scheme. Here we have adopted an Adams-Bashforth scheme. This upwinding process can also be used to impose the characteristic boundary conditions through the flux at the ends of the global domain Ω.

2.2.1 Boundary Conditions

The analytic hyperbolic system and its discretisation require appropriate boundary conditions at the inflows and these are imposed through the characteristic representation of the system. The subsonic nature of the problem means that an inlet condition is required at all boundaries of the domain. At the top of the arterial tree, for example at the heart, we can choose to set a prescribed value of velocity u, or area A, which means that this boundary acts as a reflector for outgoing waves. Alternatively, given a variation in time of velocity u and area A we can determine the variation of the incoming characteristic $W_1(t)$ and impose this value through the upwinded flux in the discontinuous Galerkin formulation. This type of boundary condition acts as a pure absorber to outgoing waves. At the periphery of the arterial tree we typically prescribe a reflection condition [18, 10], where the incoming characteristic is set to be equal to the outgoing characteristic value scaled by the reflection coefficient. More details are found in Sherwin et al. [9, 10].

3 Arterial networks in placentas

3.1 Monochorionic Placentas

The one-dimensional model has been applied to the calculation of waveforms in a single fetoplacental circulation and a monochorionic twin pregnancy where two fetuses share a single placenta. In monochorionic placentas there can be anastomoses (joining routes) between blood vessels of the two fetoplacental

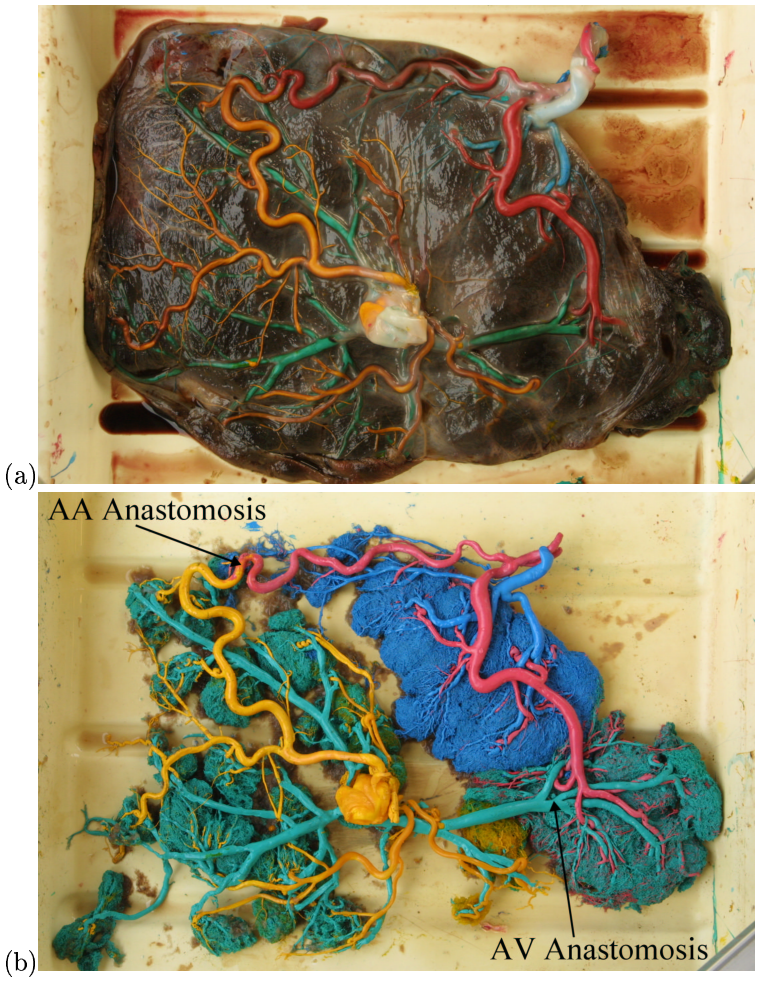

Figure 1: Figures (a) and (b) show a placenta with the plastic resin in the arterial and venous system before and after the surrounding tissue has been dissolved by hydrochloric acid. The system on the left belongs to the larger fetus and the arteries and veins are coloured yellow and green respectively, the right system belongs to the smaller fetus and the arteries and veins are coloured red and blue respectively.

circulations, which result in a transfer of blood between the two fetuses. If unbalanced transfer from one fetus to the other occurs, then one fetus receives too much blood to the detriment of the other twin. In extreme cases this can lead to a medical condition called twin-to-twin transfusion syndrome (TTTS) and can be fatal. There are three types of anastomoses that can occur in between the fetoplacental circulations: arterio-arterial anastomoses (AAA), arterio-venous anastomoses (AVA) and venous-venous anastomoses (VVA). In TTTS the fetuses are described as the donor (net outflow of blood) and recipient, but strict criteria must be met for the cases to be classified as TTTS, so to avoid confusion throughout this paper we will denote the fetuses as smaller and larger in reference to the mis-matched growth that often occurs.

In the case of a typical arterio-venous anastomosis an artery from the smaller fetus is seen to cross the surface of the placenta, it then dips under the surface and supplies blood to a cotyledon belonging to the venous system of the larger fetus. Strictly speaking it is an incorrectly connected cotyledon rather than an anastomosis. It is in the cotyledons that the exchange of oxygen, nutrients and waste products between the mother's and the fetus' blood occurs. Note that the mother's blood is entirely separate from the fetus' blood and because the placenta belongs to the fetus, the blood in the placental circulation belongs to the fetus. The blood then leaves the cotyledon through a vein belonging to the larger fetus' circulation. Blood is transfusing from the high pressure arterial system of the smaller fetus to the low pressure venous system of the larger fetus, and due to the pressure difference can only travel in this direction. It is thought that the outcome is usually worse when only arterio-venous anastomoses of a

given direction are present as there is no route for the blood to return from the larger fetus, that has too much blood, to the smaller fetus, which is now lacking in blood. With only this type of anastomosis the wave pattern often appears normal in the arteries of the placenta and the umbilical artery (i.e. non-reversing/mono-directional) and can therefore potentially go unrecognised using Doppler ultrasound as a diagnostic tool. It may however be possible to see arterio-venous anastomoses on the surface of the placenta by either colour Doppler ultrasound or endoscopy [16]. Diagnosing that TTTS is present is usually achieved from the characteristic features of the fetuses: the recipient fetus will be larger and have an elevated level of amniotic fluid, whereas the donor fetus may have almost none, is lacking in nutrients and is smaller. Where the imbalance between the fetuses is large often neither survives.

Arterio-arterial anastomoses are present in 85% of monochorionic pregnancies, but are not necessarily associated with a negative outcome for the fetuses. Indeed there is some evidence that the existence of these anastomoses may be protective, with a lower incidence of TTTS, and even if TTTS develops, a better survival than in the TTTS cases with only arterio-venous anastomoses [13, 14]. Arterio-arterial anastomoses are thought to be protective because they provide a flow path for blood to transfuse from the larger fetus back into the smaller fetus. i.e. in an AVA blood can only travel in one direction whereas in an AAA blood can travel in either direction, thus balancing the system. In a typical arterio-arterial anastomosis an artery belonging to one fetoplacental circulation connects directly with an artery belonging to the other fetoplacental circulation and does not enter a cotyledon first. This usually occurs on the surface of the placenta and can often be seen by colour Doppler ultrasound, or through an endoscope. The anastomosis connects the high pressure arterial systems of the fetuses and the blood in the anastomosis can travel in either direction depending on which fetus' blood is at the higher pressure. The waveforms in the arteries in the placenta of a healthy fetus are periodic and positive, therefore when two flows meet in opposite directions in an arterio-arterial anastomosis they produce a flow that oscillates between positive and negative velocity [17]. Typically the heart rates of the fetuses are different, which will produce a wave pattern which is repeated periodically with a frequency dependent on the difference in heart rates [17]. Venous-venous anastomoses are rare and maybe associated with a lower survival [3].

In the following results we have concentrated on modelling a network with an arterio-arterial anastomosis, because we are interested in predicting and understanding the unusual reversing periodic waveform seen in this vessel using Doppler ultrasound. We have modelled only the arterial side, the venous side has been modelled by applying terminal reflection coefficients. These are typically low since there are small vessels and cotyledons in between the arterial and venous system which damp-out and absorb waves making the flow in this region appear relatively steady.

3.2 Placental Model

The placental topology and dimensions for the numerical model were obtained by casting placentas using Batson's casting resin. Dyed resin was injected into the arteries and veins of the placenta, figure 1(a). The resin was coloured to distinguish between the two fetoplacental circulations and the arterial (red and yellow) and venous (blue and green) systems. Once the resin had cured the placenta was placed in a basin of hydrochloric acid for several days to dissolve the surrounding tissue. Measurements were then made of the resulting cast, figure 1 (b), to determine the lengths and diameters of the arteries found in the fetoplacental circulation and the connectivity of the blood vessels was observed. The measured data for the above placenta is presented in appendix A and the connectivity is shown in figure 2.

In this particular system there is a very large arterio-venous anastomosis (red-green connection) from the smaller fetus' artery (red) via a cotyledon to the larger fetus' vein (green). There is also a large arterio-arterial anastomosis (red-yellow connection) present where blood can travel in either direction. It can be seen from figure 1(a) that the two arteries meet on the surface of the placenta whereas the artery-vein connection cannot be seen on the surface and can only be seen once the surrounding tissue has been removed, figure 1(b).

Characteristic features of the fetoplacental circulation can be seen in figure 1: the joining of the two umbilical arteries and just one umbilical vein. It can also be seen that the arterial system is usually formed on top of the venous system. Several placentas have been cast and the corresponding Doppler

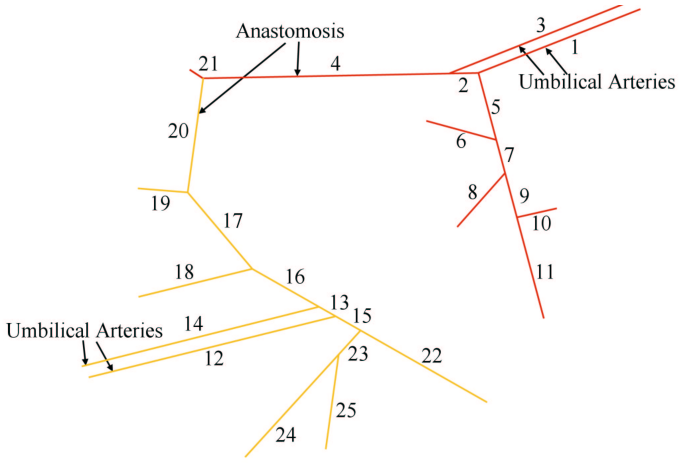

Figure 2: Connectivity of the arterial intertwin placenta network.

ultrasound waveforms obtained, however for this paper we concentrate on the placenta described in the figures.

Although this placenta belonged to two fetuses, which did not develop twin-to-twin transfusion syndrome (TTTS), the fetus on the left hand side was larger due to the intertwin transfusion. The modelling of this placenta is partcularly interesting because it has quite an extreme case of connecting arteries between the two fetoplacental circulations, i.e. the very large AVA and AAA, and if the imbalances were increased then this may have lead to twin-to-twin transfusion syndrome. The effects of a number of different parameters on the flow and pressure waveforms and the volume fluxes are studied in this monochorionic placenta.

Figure 2 shows the connectivity of the arteries for the numerical model and is at a similar orientation to the placenta in figures 1(a) and (b). Arteries 1 & 3 and 12 & 14 are the pairs of the umbilical arteries belonging to the two fetuses. Arteries 2 and 13 represent the umbilical artery anastomoses. Unfortunately when casting the placentas the umbilical cord for the left hand side fetus had to be cut down so we were unable to cast the umbilical arteries of this fetus. We therefore used the measurements of the umbilical arteries from the right hand side fetus for both systems. The inputs to the system are through these umbilical arteries.

Several assumptions have been made in order to model the arterial fetoplacental circulation. As far as we know, there is no published data on the mechanical properties of the large arteries in the placenta and we have therefore assumed that they are similar in properties to comparably sized systemic arteries. The wall thicknesses of the arteries found in the placenta are taken to be 10 percent of the vessel radius and the Young's modulus, E, is assumed to be 400 kPa throughout. The terminal resistance in the placenta is thought to be low, so we have initially modelled the system with zero terminal resistance. The density is assumed to be $1021 kg/m^3$. The input wave was imposed by specifying the W_1 characteristic at the umbilical arteries making this boundary a pure absorber. An inflow profile of a half sine squared wave over half a period was applied, i.e.

$$W_1 = u_0 + 4c, c = \sqrt{\frac{\beta}{2\rho}} A^{1/4}, A(t) = A_0 + \Delta A * \delta^2(t) H(\delta(t)) \tag{23}$$

where

$$\delta = sin(2\pi t/T),$$

and u_0 is a reference initial velocity, A_0 is the initial value of the area of the umbilical artery, see appendix A, ΔA is the maximum change in characteristic area and is calculated from the maximum change in pressure from equation 3, $H(\delta(t))$ is the Heaviside step function and T is the period of the cardiac cycle.

The time period for the calculations is 0.5 which corresponds to a heart rate of 120 b.p.m. and the aortic valve being open for 0.25 seconds. Note that in a normal fetus the heart rate is typically in the range of 110 b.p.m. to 150 b.p.m., considerably higher than that in an adult. The change in pressure over the waveform has been taken as $800Pa$. As previously discussed, at the ends of the arterial tree a terminal reflection coefficient, R_f, was applied where a value of $R_f = 0$ implies a completely absorbing boundary and a value of $R_f = 1$ implies a pure reflector.

The reflection coefficients at the bifurcations for forward travelling waves have been calculated from linear theory, the derivation of which is given in [10], and are shown in table 1. The equation to calculate the reflection coefficients in the network can be simplified to equation (24) because we have assumed density, ρ and wave-speed, c, are constant throughout the placenta.

$$R_c = \frac{A_0 - A_1 - A_2}{A_0 + A_1 + A_2} \tag{24}$$

3.3 Single placenta waveforms

Before analysing a monochorionic placenta with anastomoses it is instructive to consider the waveforms found in a single placenta. Typically in a healthy fetus the waveform found in the umbilical arteries is of the form shown in figure 3 (a). To examine the properties of our placenta we have modelled our intertwin network as two separate systems using equation (23) as our input. We have used the two fetoplacental circulations shown in figure 2 but have not connected arteries 4 and 20 at artery 21, therefore no anastomoses are present and the networks can be considered as a pair of single placentas. This allows comparisons to be made between the numerical results and those observed in a healthy fetal circulation of a single placenta, figure 3, as well as the intertwin network.

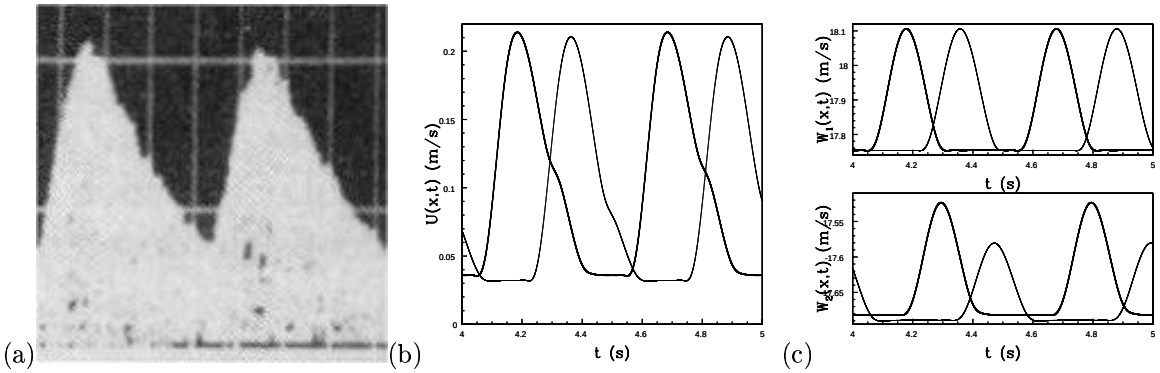

Figure 3: (a) An ultrasound Doppler flow waveform in an healthy fetus [8]. Calculated velocity waveform (b) and characteristic variables W_1 and W_2 (c) using our one-dimensional wave propagation code. The left hand side network is the bold line and the right hand side network is the thin line in the plots.

Figures 3(b) and (c) are velocity waveforms for the two unconnected systems at the mid-point in the umbilical arteries 1 (bold line) and 12 (lighter line). The input time period in the left hand side network has been changed to $T = 12/23$ which is equivalent to 115 b.p.m. The heart rate in the right hand side network is 120 b.p.m.. The velocity waveforms are shown in figure 3(b) and similarities are seen with the clinical results in figure 3(a). The flow is periodic and mono-directional i.e. no negative flow, but although in our results the velocity does decline more slowly than it increases this is not in an identical manner to that seen in a healthy fetus. This is not unexpected since the half sine squared wave used as the input to the system is only an approximation to the physiological conditions. However as we do not know the physiological waveform for these cases and they will vary from placenta to placenta we use this simplified input waveform as we believe that it captures most of the relevant physiological features. We have used a number of different input waves and the results are all similar. The waveforms in the umbilical arteries in these single networks may also not be exactly the same as a healthy waveform, because these placental arterial systems may have developed slightly differently because of the presence of the anastomoses.

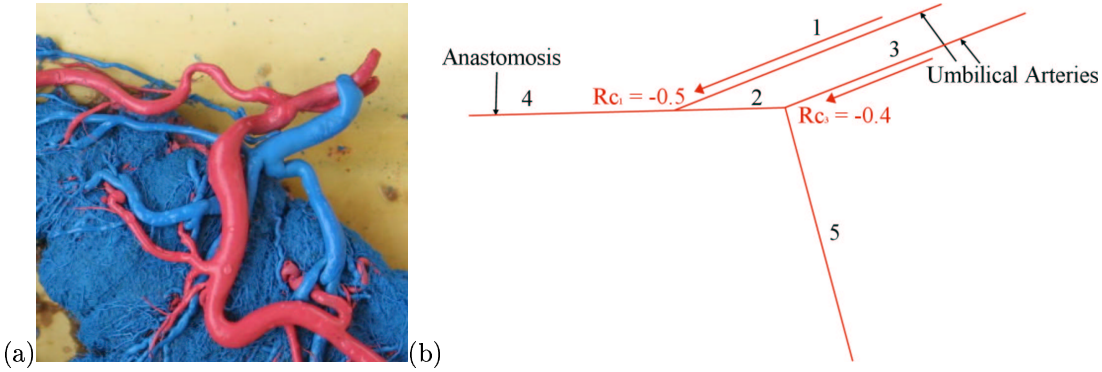

Figure 4: (a) Resin cast of the umbilical artery. (b) Reflection coefficients in the umbilical arteries for forward travelling waves.

The characteristic variables W_1 and W_2 are shown for the umbilical arteries in figure 3(c). The top figure shows the forward travelling characteristic, W_1, which is the input to the system only, because the inflows have been modelled as pure absorbers so there are no reflections. The bottom figure shows the backwards travelling wave, W_2, which is produced by the reflections occurring in the system. Even though both the systems have no terminal resistance reflections still occurred and must have been produced by the bifurcations in the network. Although we are using a non-linear model for wave propagation it was shown [10] that the differences between the linear and non-linear solutions are less than 10% and that it is reasonable to use the linear theory to calculate the reflection coefficients at the bifurcations. These were calculated for forward travelling waves throughout the whole network. It was found that the largest coefficients were those at the end of the umbilical arteries where they meet the placenta. The bifurcations further down the network are fairly well-matched, see appendix A. Figure 4(a) shows the resin cast of the umbilical arteries found in the placenta and figure 4(b) shows the connectivity of the arteries and the reflection coefficients for forward travelling waves at the ends of arteries 1 and 3. The reflection coefficients are -0.5 and -0.4 for a wave travelling as indicated at the bifurcation where the umbilical artery meets the arteries in the placenta. Note that due to the umbilical arterial anastomosis it is impossible to have all the arteries in the placenta well-matched for forward waves.

3.3.1 Terminal resistance

In the placenta it is thought that terminal resistance is low, which would be consistent with the observation of no reversed flow in the umbilical arteries of a healthy fetus. It is also thought that when a fetus is unhealthy the terminal resistance in the placenta is higher [8] and reversed flow is often seen in the umbilical artery as shown in figure 5(a).

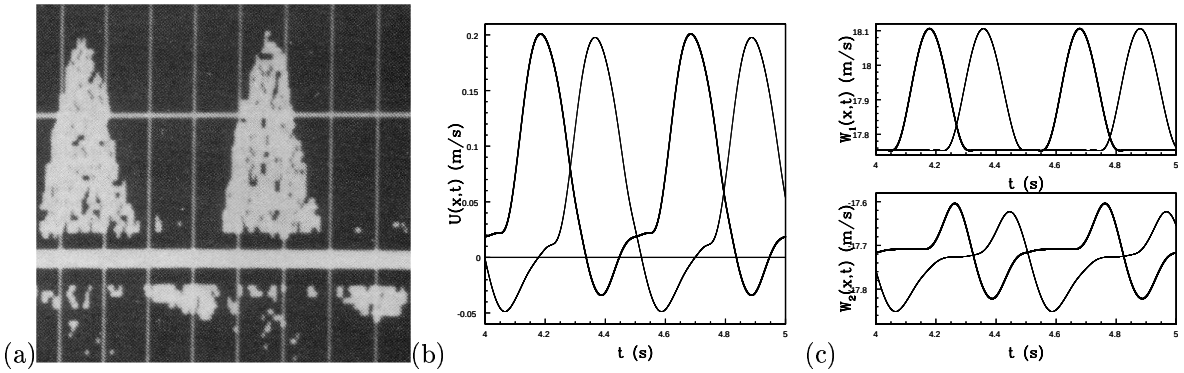

Figure 5: Effect of increasing terminal resistance in a single placenta. (a)An ultrasound Doppler flow waveform in an unhealthy fetus [8]. Calculated velocity waveform (b) and characteristic variables W_1 and W_2 (c) using our one-dimensional wave propagation code. The left hand side network is the bold line and the right hand side network is the thin line in the plots.

To simulate the terminal resistance a reflection coefficient of 0.5 has been imposed in the two networks. The waveforms found in the umbilical arteries have been calculated and are shown in figures 5(b) and (c) which are velocity waveforms taken at the mid-point of the umbilical arteries 1 (bold line) and 12 (thin line). The velocity plot, figure 5(b), shows that there is reversed flow in the umbilical artery which is similar to that seen using Doppler ultrasound in an unhealthy growth-restricted fetus with placental pathology, figure 5(a). The characteristic variables are shown in figure 5(c) and it can be seen that the W_2 characteristic firstly increases due to reflections from the bifurcation, similar to figure 3(c), but then decreases due to the system having a reflection coefficient of 0.5 at the end of the placental network causing a negative backward W_2 wave. This decrease in W_2 has a subtractive effect on the velocity waveform (see equation (13)) and hence reversed flow results. This demonstrates that the reversed flow seen in the placenta of compromised fetuses can be produced by an increase in terminal resistance of the placenta.

3.4 Monochorionic placenta waveforms

The computations for the connected network were performed for the monochorionic placental network shown in figure 2. The input to the system was imposed as a half sine squared wave through the W_1 characteristic, i.e. equation (23) was imposed at arteries 1, 3, 12 and 14. The heart rates of both fetuses were assumed to be the same with $T = 0.5$ (120 b.p.m.). The change in characteristic area in the input wave has a corresponding change in pressure of 800 Pa. Initially the terminal resistance in the system was zero. The two fetoplacental networks join at arteries 4 and 20 (the anastomoses) and have the same area and wall properties. Using the principle of Occam, we have no evidence that the arteries in the two fetoplacental circulations are different and so we adopt the simplest assumption that they are the same. Artery 21 in the network has a very small area and the reflection coefficient at the end of the vessel is equal to one. It is included in the model merely to join the two networks together and only has a very small flow which has a negligible effect on the results in the rest of the system. The volume fluxes into and out of the larger and smaller fetuses and through the arterio-arterial anastomosis have been calculated and are shown in table 1. The volume fluxes are of interest because we can calculate whether the smaller and larger fetoplacental circulation systems balance. In later computations various parameters are altered and the volume fluxes for these systems are also shown in table 1. In calculating the volume fluxes we note that artery 11 is assumed to be an arterio-venous anastomosis (AVA) and therefore connects to a vein in the larger fetus' circulation.

The velocity waveforms in the umbilical arteries and the anastomosis are shown in figures 6 (a) and (c) and the characteristic variables, W_1 and W_2, are shown in figures 6 (b) and (d). Results are shown in figures 6 (a) and (b) for the umbilical arteries 1 (bold line) and 12 (thin line) at the mid-point in the arteries. The magnitudes of the velocities in figure 6 (a), have decreased slightly when compared with the equivalent plots for the unconnected networks, figure 3 (b). This is due to the small change in magnitude in the W_2 characteristic, figure 6 (b). Again no reversed flow is present and the waveforms are similar in the two fetuses. Figures 6 (c) and (d) are the velocity waveforms taken at the ends of arteries 4 (bold line) and 20 (thin line), i.e. where the two arteries meet. The plots of arteries 4 and 20 at this point show the same results but the reference for positive and negative flow is in the opposite direction i.e. the flow in the end of artery 4 shows negative flow and blood is flowing towards the right hand side fetus (smaller fetus) and the flow at the end of artery 20 shows positive flow which also indicates that the blood is flowing towards the right hand side fetus (smaller fetus). In the characteristic plot it can be seen that the W_1 wave for the right hand side system, artery 4, has the same waveform as the W_2 wave in the left hand side system, artery 20, but has the opposite sign and vice versa for the other two variables. Since the heart rates of the fetuses are identical the waves in each period are identical to one another and only one period needs to be studied.

The volume flux for this system is shown in the first column of table 1. In determining the flux recall that the outflow from the placenta to the smaller fetus comprises arteries 6, 8 and 10 whereas the outflow from the placenta to the larger fetus include arteries 18, 19, 22, 24 and 25 as well as artery 11 which is an AVA. From these calculations we note that there is a net flux of 0.062 litres per minute from the smaller fetus i.e. more blood is leaving the fetus through the umbilical arteries (1 and 3) than is actually returning to the fetus through the arteries (6, 8 and 10) that supply the venous system of the smaller

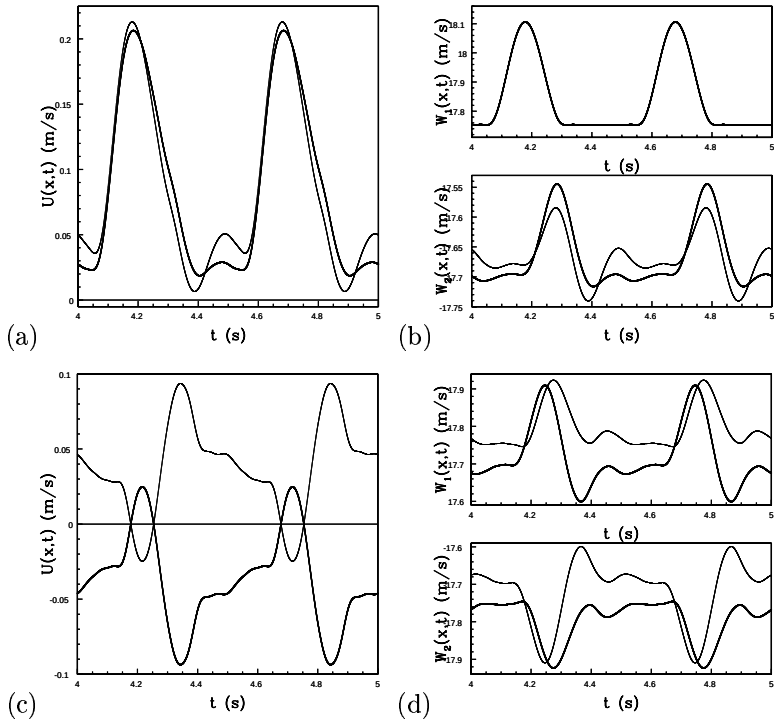

Figure 6: Calculated waveforms in the monochorionic network, with the same time period. (a) and (b) the velocity and characteristic variables, W_1 and W_2, in the umbilical arteries 1 (bold line) and 12 (thin line), (c) and (d) the velocity and characteristic variables, W_1 and W_2, in the arterio-arterial anastomosis 4 (bold line) and 20 (thin line).

fetus. The larger fetus gains blood at a rate of 0.062 litres per minute. From a numerical point of view we observe that the overall fluxes in and out of the placenta balance to within 1×10^{-7} litres per minute. Since this system does not balance it clearly cannot represent the in-vivo situation. In later sections we investigate the effect of varying other parameters, such as terminal resistance and the input pressures into the networks on the balance between the systems.

It is interesting to note that the total volume flux out of the right hand side network when the arterio-venous anastomosis is included (arteries 6, 8, 10 and also 11 this time) is larger than that from the left hand side. There is therefore a net flux through the arterio-arterial anastomosis from the larger fetus' side to the net smaller fetus' side. All the parameters are the same for the system i.e. input pressure (similar output fluxes), properties and zero terminal resistance, except the size and the connectivity of the arteries in the two fetoplacental circulations. This suggests that the connectivity and dimensions of the arteries affects the transfusion of the blood and for this particular placenta the arteries may have developed in such a manner that they help blood transfuse back from the larger fetus to the smaller fetus through the arterio-arterial anastomosis. This effect alone is not adequate to balance the systems as the arterio-venous anastomosis (artery 11) is so large and transfuses much of the blood from the right hand side into the venous system of the left hand side. In fact in this system there is more blood leaving the right hand side network through artery 11 to the larger fetus than is leaving arteries 6, 8 and 10 to the smaller fetus.

In-vivo the fetuses often have slightly different heart rates, which produces a flow waveform that varies in time as the two hearts go in and out of synchronicity. Figure 7 shows a Doppler ultrasound waveform in the arterio-arterial anastomosis of this intertwin pregnancy. In this waveform the pattern is repeated approximately every 24 cycles with the frequency related to the difference in the heart rates. The flow in the anastomosis also alternates in direction, which is not seen in arteries in the normal placenta.

To simulate this phenomenon, the time period, T, in the input equation (23) has been changed to 12/23 for the larger fetus, which is equivalent to a heart rate of 115 b.p.m.. As for the previous cases the smaller

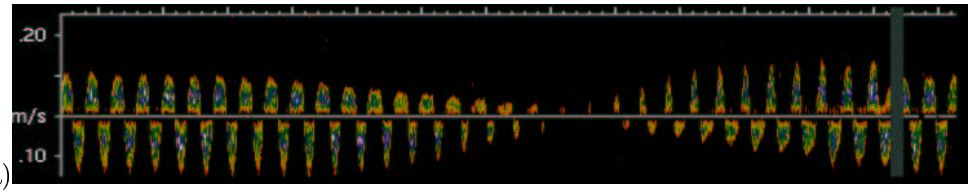

(a)

Figure 7: A flow waveform in an arterio-arterial anastomosis obtained using a Doppler ultrasound flow probe.

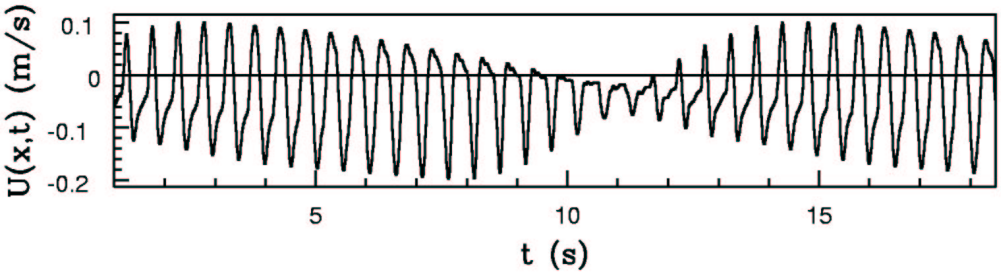

(a)

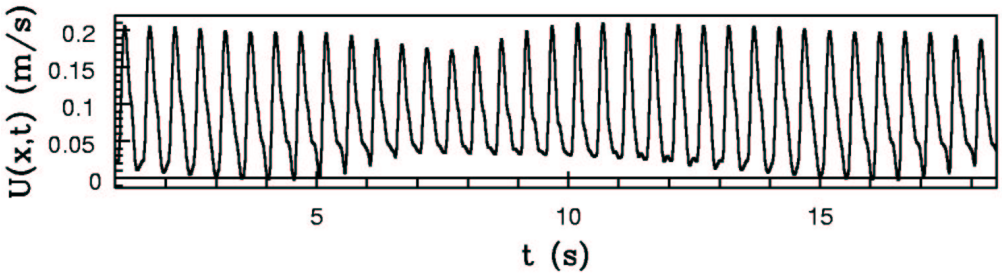

(b)

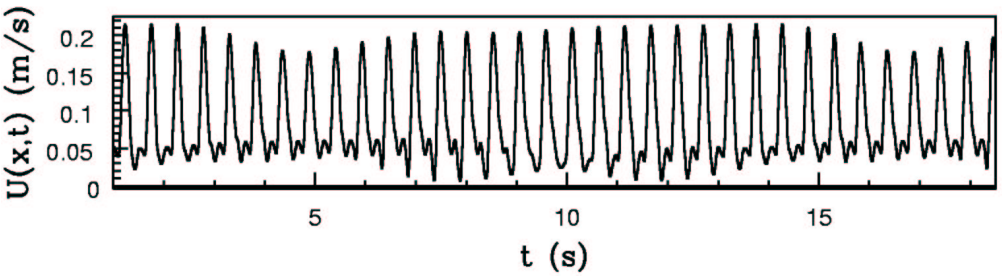

(c)

Figure 8: Effect of altering the time period in the two fetuses' input. Predicted velocity waveforms from the one-dimensional mathematical model at the end of the anastomosis, (a), artery 4. (b) and (c) velocity waveforms at the start of the umbilical arteries 1 (smaller fetus) and 12 (larger fetus).

	1	2	3	4	5	6
Volume Fluxes (litres per minute)	Same input Same period	Same input Different period	Increase input from larger fetus	Increase TR on larger fetus	Pressure and TR diff	Reduce area of AAA
Input flux into placenta from smaller fetus $u_1A_1 + u_3A_3 =$	0.134	0.134	0.099	0.099	0.084	0.141
Output flux from placenta into smaller fetus $u_6A_6 + u_8A_8 + u_{10}A_{10} =$	0.072	0.072	0.072	0.103	0.085	0.066
Net Flux Smaller Fetus Output - Input Flux =	**−0.062**	**−0.062**	**−0.026**	**0.0041**	**0.0005**	**−0.075**
Input flux into placenta from larger fetus $u_{12}A_{12} + u_{14}A_{14} =$	0.134	0.134	0.170	0.099	0.156	0.141
Output flux from placenta into larger fetus $u_{18}A_{18} + u_{19}A_{19} + u_{22}A_{22} +$ $u_{24}A_{24} + u_{25}A_{25} =$	0.105	0.105	0.105	0.051	0.084	0.134
$u_{11}A_{11}(AVanastomosis) =$	0.091	0.091	0.091	0.044	0.072	0.083
Net Flux Larger fetus Output - Input Flux =	**0.062**	**0.062**	**0.026**	**−0.0041**	**−0.0005**	**0.075**
Flux through AA Anastomosis $u_4A_4 =$	-0.029	-0.029	-0.064	-0.048	-0.072	-0.0077

Table 1: Table of fluxes in the intertwin network. The effect of varying different parameters in the network.

fetus was modelled with a heart rate of 120 b.p.m.. Figure 8(a) shows the results in the anastomosis (artery 4) and figures 8(b) and (c) show the results in the umbilical arteries (1 and 12 respectively). The waveform in figure 8(a) repeats every 24 cycles and the velocity changes in a similar manner to the Doppler ultrasound flow-probe waveform obtained in-vivo.

In the previous example both the period and the phase were assumed to be exactly the same for both the larger and the smaller fetuses. The velocity plots shown in figures 6(a) and (c) are the resultant velocity waveforms calculated from equation (13) and are exactly the same for every period. When the heart rates are different the alignment of W_1 and W_2 in the anastomosis is not the same for each period and hence the resultant velocity waveform is slightly altered with each cycle. After 12 seconds, which is 24 cycles of the faster heart rate and 23 cycles of the slower heart rate, the characteristics are once again in the same alignment as for the first cycle. The different heart rates cause the velocity waveform to alternate in direction. At approximately $t = 11$ in figure 8(a) the characteristic variables W_1 and W_2 in the anastomosis are in phase and tend to cancel each other, which results in a small velocity. Similarly at approximately $t = 5$ the magnitudes of the velocity in the anastomosis are largest since W_1 and W_2 are out of phase and reinforce one another.

The umbilical artery velocity plots in figures 8 (b) and (c) are also periodic with the pattern repeated every 24 cycles, but the differences between successive velocity waveforms are not as pronounced as those seen in the anastomosis. This is because the input wave is the dominant feature and there is more influence from other reflections occurring in the system i.e. from bifurcations at the umbilical artery, which produce backward travelling waves with the same period as the input W_1 characteristic. Reversed flow is now seen in the umbilical artery of the smaller fetus. In-vivo, reversed flow is typically only seen in the smaller fetus. The volume flux in the arteries varies for consective heart beats, therefore

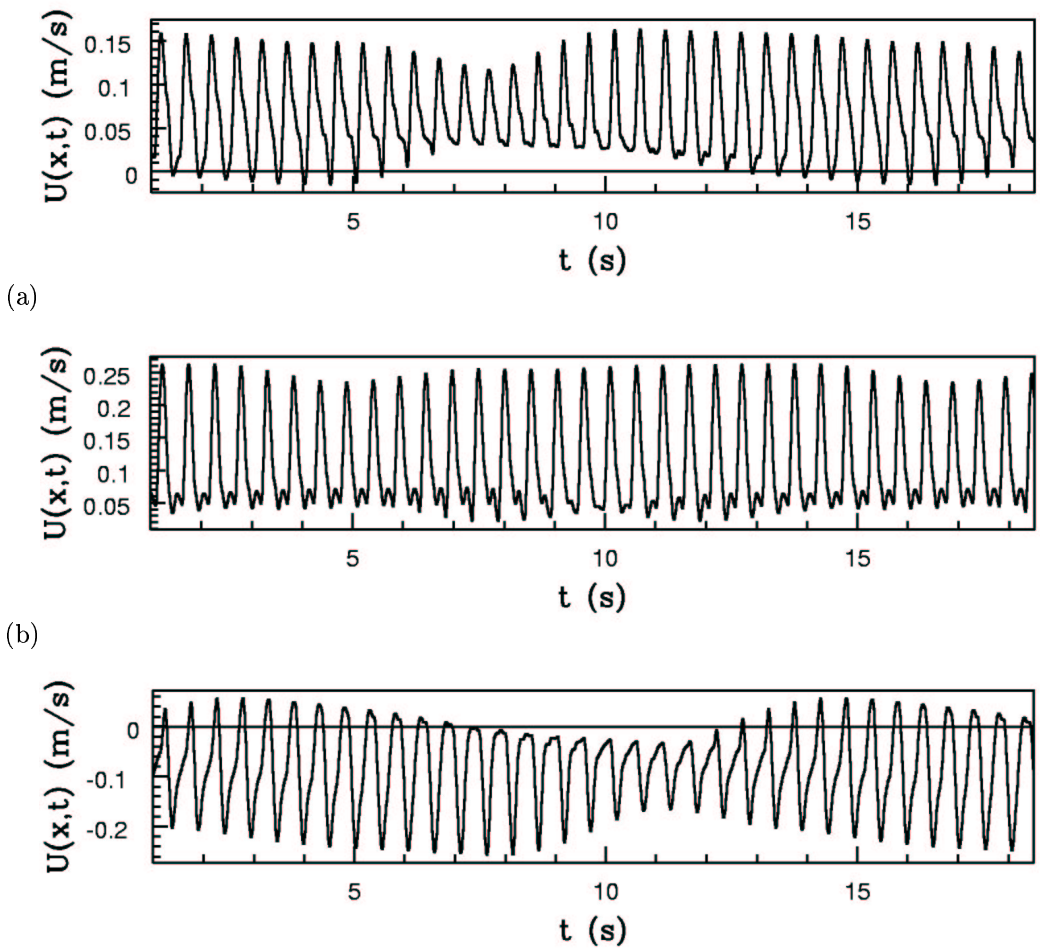

Figure 9: The effect of altering the magnitude of the input pressures. Predicted velocity waveforms from the one-dimensional mathematical model in (a) and (b) the umbilical arteries 1 (smaller fetus) and 12 (larger fetus) and (c) the anastomosis, artery 4.

the average volume flux is calculated from an entire cycle of the periodic pattern and in this case is 24 heartbeats. Changing the heart rate has little effect on the time averaged net fluxes in and out of the placenta.

It should also be noted that if the difference between the heart rates of the two fetuses is very small the Doppler ultrasound measurements may be misinterpreted due to the time required for the characteristic periodic pattern to repeat. If the observation period is too short then the magnitudes of successive waves may not appear to differ and waveforms with all positive flow, or all with some negative flow may be seen. The waveform observed depends on the relative phase of the two heartbeats thus the interpretation may differ accordingly.

3.4.1 Different inputs

Often the smaller fetus is weaker than the larger fetus and the reversing periodic pattern is only seen in the smaller fetus' umbilical artery. For the placental system considered there was indeed a larger fetus. During gestation it was overloaded with blood and thus received more oxygen and nutrients than the under supplied smaller fetus and therefore grew more. The excess blood in the larger fetus increases its venous blood pressure, its heart has to work far harder to pump the excess blood and the excess waste products can accumulate in the larger fetus. Indeed clinically, it is often the larger fetus which does not survive [19].

To model the effect of the different sized fetuses, we have increased the change in pressure to 1000 Pa in the larger fetus and decreased the change in pressure to 600 Pa in the smaller fetus. These are extreme values for the difference in pressures so that we can easily assess the effects. The results illustrate the effect that differing input pressures in the umbilical arteries have on the waveforms and volume fluxes in the system. The waveforms in the umbilical arteries are shown in figures 9 (a) and (b). The smaller fetus, figure 9 (a), has negative flow in its umbilical artery and its velocity magnitude appears to oscillate more than in the previous example, figure 8 (b). This is because the magnitude of the input characteristic, W_1, has been reduced and the influence from the larger fetus through the W_2 characteristic is therefore greater. In contrast the larger fetus' velocity plot, figure 9 (b), has all positive flow and the magnitude does not oscillate as much as it did previously, figure 8 (c), because this fetus has a greater W_1 input and the influence from the smaller fetus is less significant. This waveform looks more like a normal single placental waveform and is commonly seen in the umbilical arteries of the larger fetuses. In the anastomosis, figure 9 (c), the flow is more negative and the velocity magnitude does not vary as much as in the previous case. The fluxes for this system are shown in column 3 of table 1. The volume fluxes returning to the fetuses have not changed significantly, although the imposed volume flux has increased for the larger fetus and has decreased in the smaller fetus. This difference has been overcome by a large increase of 0.064 litres per minute through the anastomosis. The balance of volume flux in and out of the fetuses has also improved, the difference is now only 0.026 litres per minute which means that this arrangement is closer to the physiological case than the previous case where the inputs were the same. This has occurred however because the smaller fetus' input has now decreased and not because there is a reduced flow through the arterio-venous anastomosis.

3.4.2 Terminal resistance

The presence of the arterio-venous anastomosis in the modelled fetoplacental circulation means that there is a tendency for blood to be transfused from the smaller fetus to the larger fetus, as we have seen in the previous sections, but there is only a limited blood capacity in the larger fetus' circulation and the blood pressure will rise which will affect the flow patterns. To simulate this effect we have applied a terminal resistance to the terminal vessels belonging to the larger fetus by imposing a reflection coefficient of 0.5. These are arteries 18, 19, 22, 24, 25 and also artery 11, which although it belongs to the smaller fetus, is part of the arterio-venous anastomosis and so connects with a vein belonging to the larger fetus. The pressure change for both inputs has been modelled as 800 Pa.

The volume fluxes in the system are shown in column 4 of table 1. For this configuration the volume fluxes in and out of the smaller and larger fetuses are approximately the same, therefore the systems are nearly balanced. This has occurred due to both the volume flux increasing through the arterio-arterial anastomosis and decreasing through the arterio-venous anastomosis, so they are now approximately equal, which is essential for the systems to balance. The total volume flux returning to the larger fetus has decreased due to the increase in terminal resistance. Comparing the system with no terminal resistance in the larger fetus' fetoplacental circulation, table 1 column 2, with this system with terminal resistance, there is now more blood returning to the smaller fetus from arteries 6, 8 and 10 than transfusing to the larger fetus through artery 11.

An increase in terminal resistance has also caused a large reduction in volume flux into the placentas of both the larger and smaller fetus, which may not be representative. We would need to model the entire circulation including the two fetuses to determine the real effect on the placental circulations relative to the fetal circulations. With the improved algorithms we are using, there is no reason why we could not include many more vessels into the model, if the data were available for the fetal circulations. However the vast number of vessels in the microcirculation means that solving the entire circulation would be computationally expensive, therefore it would be more attractive to model this through multiscale techniques, as proposed by Formaggia et al. [5] and Smith et al. [12], where the 1D model is coupled to a lumped 0D model which represents the smallest vessels. We have actually done some preliminary work on modelling the smaller arteries and the arterioles as a fractal structure using recursive techniques to determine the transfer function for the fractal. Eventually we would like to incorporate these ideas into an improved model of the circulation where the microcirculation was not modelled as a simple resistance. However, this approach still needs development and validation.

Figures 10 (a) and (b) show the velocity waveforms at the mid-points of the umbilical arteries 1 and

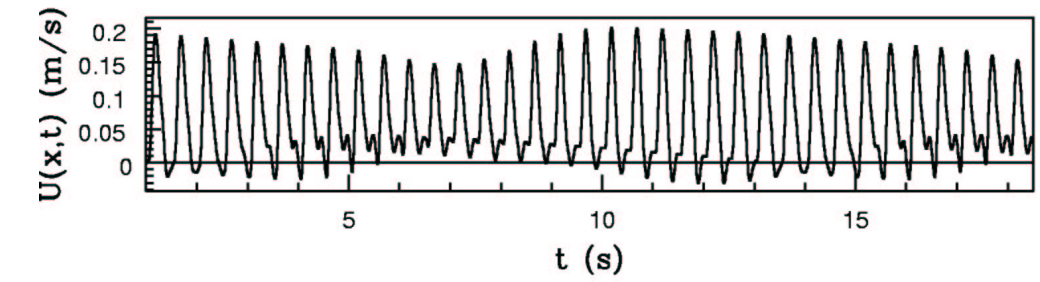

(a)

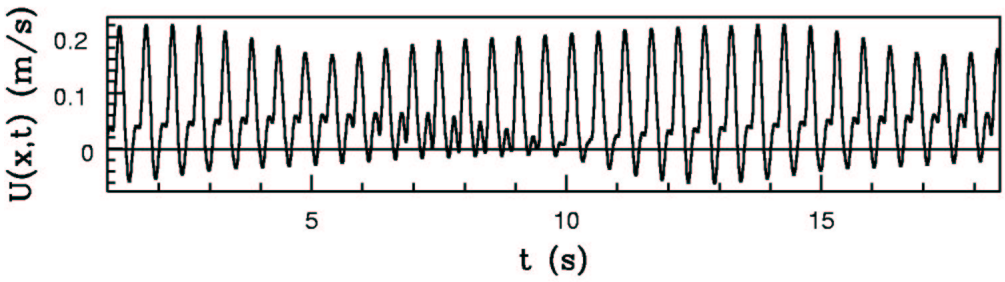

(b)

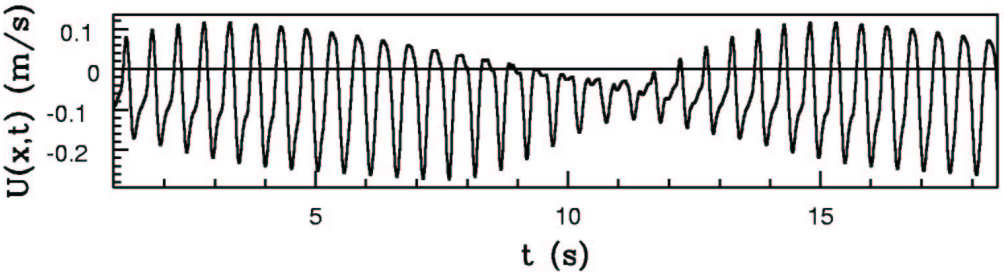

(c)

Figure 10: The effect of adding terminal resistance to the placental circulation of the larger fetus. Predicted velocity waveforms in (a) and (b) the umbilical arteries, 1 (smaller fetus) and 12 (larger fetus) and (c) the anastomosis, artery 4.

12. In both of these plots there is negative flow and the magnitudes vary due to a large influence from the other fetus. As mentioned earlier, reversed flow is often only seen in the smaller fetuses umbilical artery, therefore in the previous example the velocity plots, figure 9 (b), were more appropriate for physiological conditions. The flow in the anastomosis is shown in figure 10 (c) and the waveform looks very similar to figure 8 (a), but the velocity magnitudes are greater due to the increase in volume flux. These waveforms indicate that the choice of a reflection coefficient of 0.5 in this example is probably too large.

In the previous system it was shown that increasing the output from the larger fetus helped to balance the fetal circulations and in this section that increasing the terminal resistance on the larger fetus also balances the circulations, but neither effect balances the system in a physiological manner. In-vivo, there is a complex interaction between arterial blood pressure and the resistance of the microcirculation which is beyond the capability of our simple model to predict. Our results however, do indicate that it is probably more realistic to model the network with both a higher terminal resistance on the larger and an increase in the input to larger fetus' placental circulation.

The results of combining different input pressures and an elevated terminal resistance for the larger fetus' circulation are shown in figure 11. In this system, input pressures of 600 Pa and 1000 Pa and a reflection coefficient of 0.2 on the larger fetus have been used. The velocity waveform in the smaller fetus' umbilical artery has a periodically negative flow, figure 11 (a), and the flow waveforms in figure 11 (b)

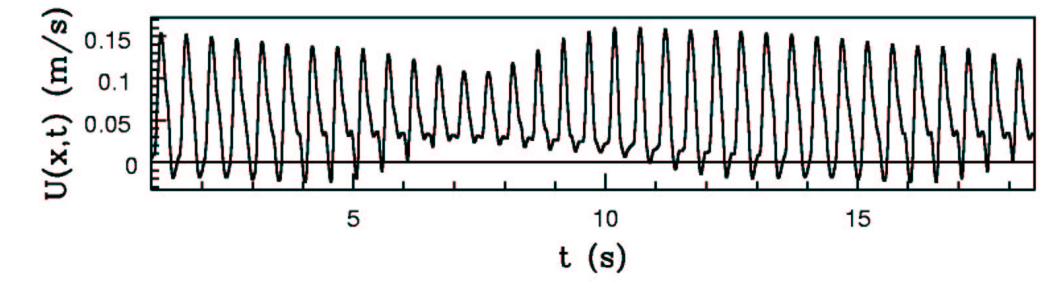

(a)

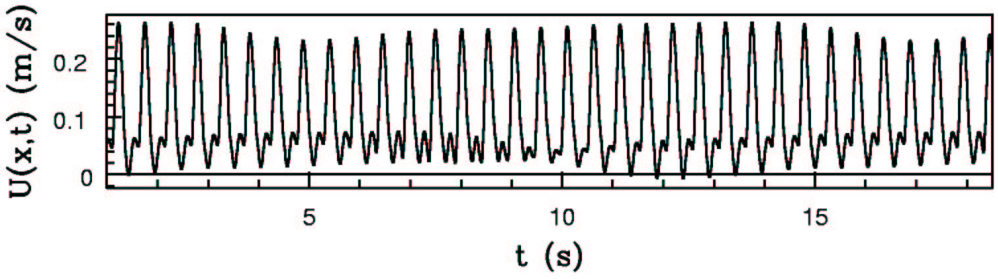

(b)

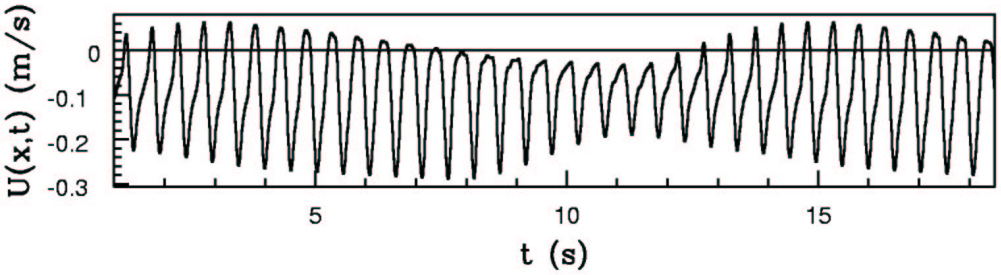

(c)

Figure 11: The effect of altering pressure to 600 and 1000 Pa in the smaller and larger fetus respectively and a reflection coefficient of 0.2 in the larger fetus. Predicted velocity waveforms in (a) and (b) the umbilical arteries, 1 (smaller fetus) and 12 (larger fetus) and (c) the anastomosis, artery 4.

for the larger fetus now appears positive, similar to what is observed from in-vivo Doppler ultrasound waveforms. The volume fluxes for this case are very nearly balanced and the flow in the anastomosis is also similar to that seen in the Doppler ultrasound measurements. The general patterns are therefore very encouraging although the precise form of each wave is not identical to the physiological case due to the simplifications and assumptions made about the network and the input conditions.

3.4.3 Anastomosis Area

In this fetoplacental circulation there is an arterio-arterial anastomosis of large cross-sectional area, but in other circulations that have been cast the arterio-arterial anastomoses are smaller. We have therefore reduced the area of the anastomosis in this case to investigate the effects a smaller conduit would have on the waveforms in the umbilical arteries. The area of the anastomosis, artery 20, was reduced to 3.14 mm^2 and the areas of arteries 19 and 21 were increased to 16.6 mm^2 and 9.62 mm^2 respectively so that all forward waves would be well-matched as before and consequently no new reflections would occur from the bifurcations.

The waveforms in the umbilical arteries are shown in figures 12(a) and (b) and it can be seen that there is no reversed flow and only a slight change in velocity magnitude between successive beats. The waveforms have not been greatly influenced by any other waves from the other fetus (characteristic variable W_2) and appear similar to those found in a normal healthy fetus, figure 3(a). The velocity

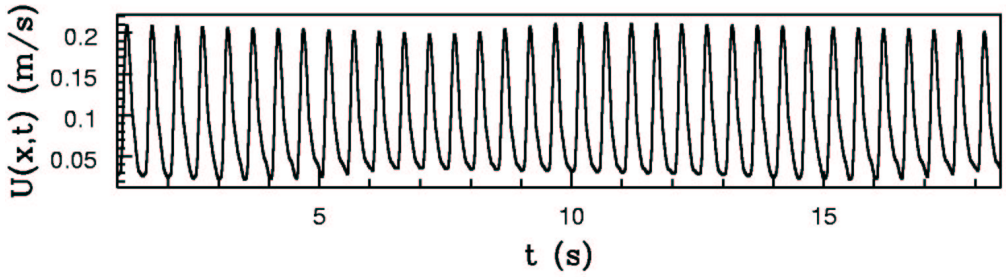

(a)

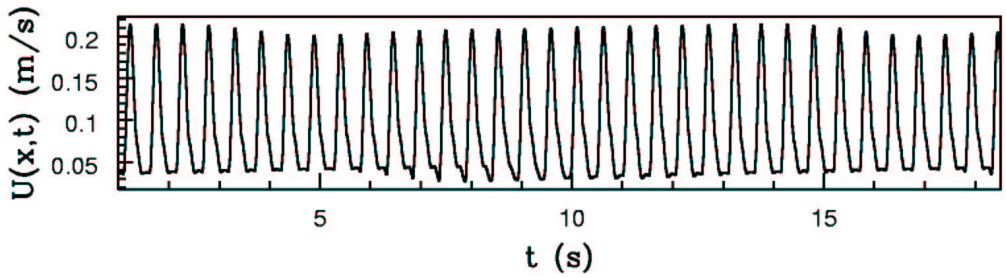

(b)

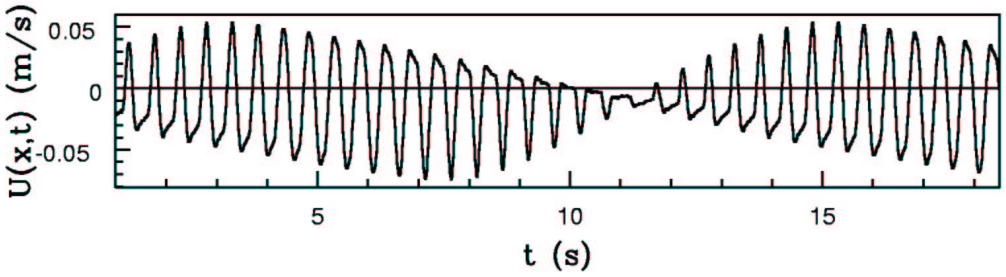

(c)

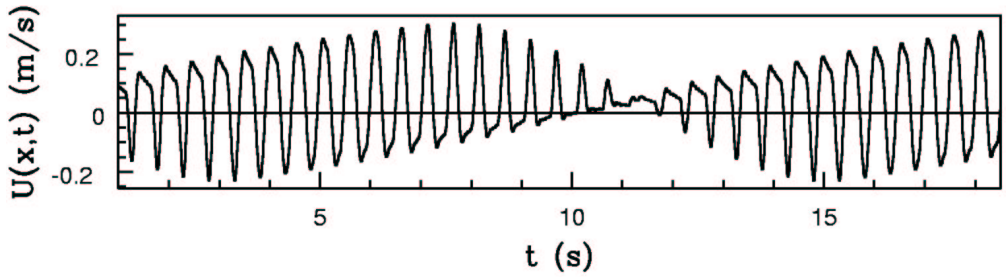

(d)

Figure 12: The effect of reducing the area of the arterio-arterial anastomosis, artery 20. Predicted velocity waveforms in (a) and (b) the umbilical arteries, 1 (smaller fetus) and 12 (larger fetus) and (c) and (d) the anastomosis, arteries 4 and 20.

waveforms in the anastomosis are shown in figures 12(c) and (d). Figure 12(c) is the velocity waveform in artery 4, which has remained the same area as the previous cases, and figure 12(d) is that in artery 20, which has been reduced in area. They both have the same periodic pattern but artery 4 is the reverse of artery 20, as for the example shown in figure 6(c). The velocity magnitude has increased in artery 20 because the area has been reduced but has decreased in artery 4 even though this artery has the same area as before. This is due to the reduction in area of the other section of the arterio-arterial anastomosis, which increases its resistance and reduces its efficiency as a flow conduit. The volume flux through the anastomosis shown in column 6 of table 1, has reduced to 0.0077 litres per minute, so hardly any blood is transfusing through this anastomosis, consequently the imbalance between the fetuses circulations is large with the smaller fetus now lacking 0.075 litres per minute. In the previous examples the arterio-arterial anastomosis was the channel for blood to transfuse to the smaller fetus, but with a small anastomosis as in this case the protective effect of the arterio-arterial anastomosis is more limited. This network is hypothetical and would probably not exist as the fetuses would not survive. From casting the placentas we have not found a case with a large arterio-venous anastomosis with only a single small arterio-arterial anastomosis. This tallies with the results of the numerical modelling and we expect that for these fetuses to survive either a large or multiple smaller arterio-arterial anastomoses or an arterio-venous anastomosis from the larger fetus to the smaller fetus would need to co-exist. It can be seen in the volume flux table, 1 colume 6, if artery 11 was not an arterio-venous anastomosis and its output was to go to the smaller fetus then these systems would be more likely to balance once other parameters have been altered.

4 Conclusion

The results obtained using the one-dimensional wave propagation code to model waveforms in arterial networks have the same main features as those observed in-vivo. This suggests that the time domain one-dimensional code is a reasonable and useful method of predicting and analysing flow waveforms and fluxes throughout fetoplacental networks. The effects of a number of different parameters on the waveforms have been considered for a fetoplacental circulation obtained by making a plastic cast of a monochorionic twin placenta where the two fetoplacental circulations are connected by an arterio-arterial anastomosis and an arterio-venous anastomosis.

For the two fetuses modelled in this paper to have survived homeostasis must have been maintained, (the existence of a stable internal environment for all organisms to survive). Homeostasis would not have been maintained if one of the fetuses had recieved too much blood. However, the twin fetuses were healthy and did survive until birth, therefore the volume fluxes in the two fetoplacental circulations must have balanced for this case.

By modelling the fetoplacental circulation in the intertwin case with different heart rates for each fetus the characteristic periodic pattern was produced. For several beats one fetus will be receiving too much blood and then vice-versa and the volume flux through the anastomosis oscillates around the average blood flow required to maintain homeostasis. The volume fluxes calculated in this paper were the averages across the phase pattern.

The magnitudes and shapes of the waveforms in the intertwin case were altered by variations in the input magnitude and the terminal resistance, but the most significant effect was on the volume fluxes. It was found that in order for the fluxes to balance in each fetus a combination of different input pressures and increased terminal resistance on the larger fetus' placental circulation was required. This combination can be justified physiologically and gave encouragingly similar waveforms in the anastomosis and umbilical cords to those seen in-vivo. The results of the intertwin studies suggest that the arterio-arterial anastomosis in this network does indeed have a 'protective' influence because it provides a flow path for blood to return to the smaller fetus' side, which reduces the effects of the flow through the large arterio-venous anastomosis. Since there is such a large volume flux through the arterio-arterial anastomosis it is clearly an important conduit in the fetoplacental circulation for this case and thus any surgical alteration to arterio-arterial anastomoses identified in intertwin placentas in-vivo should certainly not be automatic.

It was shown that when the arterio-arterial anastomosis was reduced in area then there was a very large imbalance of mass-flux in the fetoplacental circulation and the chances of the fetus' survival would be

greatly reduced. Indeed for this case the arterio-arterial anastomosis may have developed to a vessel of large cross-sectional area in order to maintain homeostasis. For other placentas which have been cast up to now the area of the arterio-arterial anastomosis has been proportionate to that of the arterio-venous anastomosis.

The sensitivity of our results to our different simplifying assumptions is very difficult to quantify, because of the large number of parameters that make up our model. We have taken "best guesses" for these parameters based upon extrapolations from what is known about adult and animal systemic circulations. We have not had to alter these in any systematic way to find the reported behaviour, which hints that the results are not particularly sensitive to most of the parameters, although, not having made a systematic study, we cannot say this for certain.

Although only one placenta has been studied in detail in this paper and more must be investigated, it does appear that useful information can be derived from the waveforms in both the umbilical arteries and any arterio-arterial anastomoses. The waveforms in the umbilical artery reveal the presence of any significant arterio-arterial anastomoses through the periodic variation in the velocity waves. Once an arterio-arterial anastomosis has been identified its waveform can be very revealing, particularly if the area can be measured and the net volume fluxes calculated. Given suitable information about the vessel area the volume fluxes could be calculated by integrating the velocity waveform obtained using a Doppler ultrasound flow probe. A high net flux indicates that there must be another significant flow conduit in the placental circulation and may indicate the presence of an arterio-venous anastomosis which are generally more difficult to identify visually.

The importance of arterio-arterial anastomoses has been recognized clinically and identical twins are already routinely scanned for their presence. The clinical implications of the presence of arterio-arterial anastomoses in monochorionic placentas is that they have been found to protect against the development of twin-twin transfusion syndrome [2, 3] in fetuses. In the few cases which develop twin-twin transfusion syndrome the fetuses with an arterio-arterial anastomosis present have a higher survival rate [15]. Clinicians are therefore of the opinion that the presence of an arterio-arterial anastomosis is advantageous and would like to understand the fluid dynamics of the system better both in general and also in specific cases.

The results described in this work are the very first results of our simplistic model of the incredibly complex arterial system. As such, we would hesitate to suggest that should form the basis of any clinical decisions. However, we do suggest that even these simple models can illuminate the reasons for clinical observations and suggest mechanisms for these observations. Eventually we hope that this sort of modelling can be improved and, more importantly, tested and validated so that it can become a clinical tool. Until then, it can only be a model which helps us interpret what is seen clinically. There are many precedents for this approach in fluid mechanics. For example, the details of flow in the regions near a wall can be very complex but understandable with knowledge of the behaviour of boundary layers in simpler, idealistic flows. We feel that the understanding of the effects of waves and their reflections and re-reflections in these idealised model networks can help us to understand the complex flows in real arterial systems.

The numerical model is also inexpensive to compute and codes based on this approach are certainly computationally feasible.

Acknowledgements

The first author would like to acknowledge financial support from an EPSRC studentship. Partial support of the work is acknowledged under EU grant HPRN-CT-2002-00270. Dr. Wee was supported by the Richard and Jack Wiseman Trust. The last author would like to acknowledge the partial support of a Global Research Award from the Royal Academy of Engineering. The authors would like to thank N. Watkins from the Bioengineering department for his help with casting the placenta.

References

[1] B. Cockburn and C.W. Shu. TVB Runge-Kutta projection discontinous Galerkin finite element methods for conservation laws II general framework. *Math. Comm.*, 52:411–435, 1989.

[2] M. L. Denbow, P. Cox, D. Talbert, and N. M. Fisk. Colour doppler energy insonation of placental vasculature in monochorionic twins: absent arterio-arterial anastomoses in association with twin-to-twin transfusion syndrome. *Br. J. Obstet. Gynecol.*, 105:760–765, 1998.

[3] N. M. Denbow, P. Cox, M. Taylor, D. M. Hammal, and N. M. Fisk. Placental angioarchitecture in monochorionic twin pregnancies: relationship to fetal growth, feto-fetal transfusion syndrome, fetofetal transfusion syndrome, and pregnancy outcome. *Am. J. Obstet. Gynecol.*, 182:417–26, 2000.

[4] L. Formaggia, F. Nobile, and A. Quarteroni. A one dimensional model for blood flow: application to vascular prosthesis. In I. Babuska, T. Miyoshi, and P.G. Ciarlet, editors, *Mathematical Modeling and Numerical Simulation in Continuum MEchanics*, volume 19 of *Lecture Notes in Computational Science and Engineering*, pages 137–153, Berlin, 2002. Springer-Verlag.

[5] L. Formaggia and A. Veneziani. Geometrical multiscale models of the cardiovascular system: from lumped parameters to 3d simulations. *VKI Lecture Series*, 2003.

[6] Pedley T. J. *The fluid mechanics of large blood vessels.*, volume First Edition. Cambridge University Press, Cambridge, 1980.

[7] I. Lomtev, C.W. Quillen, and G. Karniadakis. Spectral/*hp* methods for viscous compressible flows on unstructured 2d meshes. *J. Comp. Phys.*, 144:325–357, 1998.

[8] Wilmer W. Nichols and Michael F. O'Rourke. *McDonald's Blood Flow in Arteries. Theoretical, experimental and clinical principles.*, volume Fourth Edition. Arnold, London, 1998.

[9] S. J. Sherwin, L. Formaggia, J. Peiro, and V. Franke. Computational modelling of 1d blood flow with variable mechanical properties and its application to the simulation of wave propagation in the human arterial system. *Int. J. Numer. Meth. Fluids*, 43:673–700, 2003.

[10] S. J. Sherwin, V. Franke, J. Peiro, and K. Parker. One-dimensional modelling of a vascular network in space-time variables. *Submitted to J. of Eng. Math.*, 2003.

[11] S.J. Sherwin. Dispersion analysis of the continuous and discontinuous Galerkin formulations. In *International Symposium on Discontinuous Galerkin Methods*, 1999. Newport, RI.

[12] N. P. Smith, A. J. Pullan, and P. J. Hunter. An anatomically based model of transient coronary blood flow in the heart. *SIAM J. Appl. Math.*, 62:990–1018, 2002.

[13] T. Y. T. Tam, M. J. O. Taylor, L. Y. Wee, T. Vanderheydem, and N. M. Fisk. Modified quintero staging system for twin-twin transfusion syndrome. *Submitted to Ultrasound Obstet. Gynecol.*, 2003.

[14] M. J. O. Taylor, M. L. Denbow, K. R. Duncan, T. G. Overton, and N. M. Fisk. Anatenatal factors at diagnosis that predict outcome in twin-twin transfusion syndrome. *Am. J. Obstet. Gynecol.*, pages 1023–1028, 2000.

[15] M. J. O. Taylor, M. L. Denbow, S. Tanawattanacharoen, C. Gannon, P. Cox, and N. M. Fisk. Doppler detection of arterio-arterial anastomoses in monochorionic twins: feasibility and clinical application. *Hum. Reprod.*, 15:1632–1636, 2000.

[16] M. J. O. Taylor, D. Farquaharson, P. M. Cox, and N. M. Fisk. Identification of arterio-venous anastomoses *in vivo* in monochorionic twin pregnancies: preliminary report. *Ultrasound Obstet. Gynecol.*, 16:218–222, 2000.

[17] M. J. O. Taylor, D. G. Talbert, and N. M. Fisk. Mapping the monochorionic equator. *Ultrasound Obstet. Gynecol.*, 14:372–4, 1999.

[18] J.J. Wang and K.H. Parker. Wave propagation in a model of the arterial circulation. *Submitted to J. Biomech.*, 2002.

[19] L. Y. Wee and N. M. Fisk. The twin-twin transfusion syndrome. *Seminars Neonatology*, 7:187–202, 2002.

A Network data

Artery	Length (m)	Area (mm^2)	β $\left(M\,Pa\,m^{-1}\right)$	Reflection coefficients
1	0.5	15.6	10.1	-0.51
2	0.01	9.62	12.9	-0.40
3	0.51	9.62	12.9	-0.40
4	0.125	12.8	11.2	0.00
5	0.05	37.9	6.49	-0.11
6	0.005	10.2	12.5	N/A
7	0.04	37.4	6.54	0.04
8	0.01	3.14	22.6	N/A
9	0.02	31.2	7.16	-0.09
10	0.01	9.08	13.3	N/A
11	0.05	28.3	7.52	N/A
12	0.5	15.6	10.1	-0.32
13	0.01	9.62	12.9	-0.53
14	0.51	9.62	12.9	-0.53
15	0.05	20.4	8.85	0.00
16	0.06	21.9	8.55	-0.17
17	0.07	19.6	9.03	0.08
18	0.1	11.3	11.9	N/A
19	0.025	3.80	20.5	N/A
20	0.13	12.8	11.2	0.00
21	0.01	0.0079	451	N/A
22	0.105	6.33	15.9	N/A
23	0.03	13.9	10.7	0.11
24	0.102	7.92	14.2	N/A
25	0.41	3.24	22.2	N/A